Clinical Investigation / Araştırma

DOI: 10.4274/tjod.galenos.2026.94515

Turk J Obstet Gynecol 2026;23(1):71-80

A preliminary investigation of gene expression and levels of FSH, IL-10, and TNF-α and histological staining in natural aging mice

Doğal yaşlanan farelerde gen ifadesi ve FSH, IL-10 ve TNF-α düzeyleri ile histolojik boyama üzerine bir ön araştırma

Yulice Soraya Nur Intan[1,2], Soetrisno Soetrisno[2,3], Abdurahman Laqif[3], Dono Indarto[4,5]

[1]*Universitas Islam Sultan Agung Faculty of Medicine, Department of Obstetrics and Gynecology, Semarang, Indonesia*

[2]*Universitas Sebelas Maret Faculty of Medicine, Doctoral Program of Medical Sciences, Surakarta, Indonesia*

[3]*Universitas Sebelas Maret Faculty of Medicine, Dr. Moewardi General Hospital, Department of Obstetrics and Gynecology, Surakarta, Indonesia*

[4]*Universitas Sebelas Maret Faculty of Medicine, Department of Physiology, Surakarta, Indonesia*

[5]*Universitas Sebelas Maret Faculty of Medicine, Biomedical Laboratory, Surakarta, Indonesia*

Abstract

Objective: This study aimed to compare estrous cycle patterns, serum hormone and cytokine levels, gene expression, and ovarian morphology between healthy and aging mice, to evaluate their potential as models of reproductive aging.

Materials and Methods: Female BALB/c mice older than 9 months were used as the aged group and were compared with healthy controls (6-8 weeks old). Estrous phases were monitored for six days using vaginal cytology. Ovarian morphology was analyzed using hematoxylin and eosin staining and immunohistochemistry. Serum levels of follicle-stimulating hormone (FSH), interleukin (IL)-10, and tumor necrosis factor-alpha (TNF-α) were measured by enzyme-linked immunosorbent assay. Gene expression of IL-10 and TNF-α was assessed by reverse transcription polymerase chain reaction.

Results: Healthy mice cycled through all estrous phases, whereas aging mice were predominantly arrested in diestrus and exhibited increased immune-cell infiltration and inflammatory changes. Ovarian histology showed enlargement, fibrosis, and the presence of non-functional structures. Follicle counts were reduced in aging mice, though the reduction was not statistically significant. Serum FSH (1.37±0.20 vs. 1.10±0.03 pg/mL) and TNF-α (37.05±17.31 vs. 21.57±4.62 pg/mL) were significantly elevated, whereas IL-10 was significantly decreased (4.53±0.32 vs. 6.23±0.99 pg/mL) ($p<0.05$). TNF-α mRNA levels increased and IL-10 mRNA levels decreased; however, these changes were not statistically significant.

Conclusion: Aging BALB/c mice exhibit disrupted estrous cycles, ovarian fibrosis, increased FSH and TNF-α, and reduced IL-10, changes that resemble those associated with menopause. These findings support the use of aging BALB/c mice as a model for reproductive aging and therapeutic studies.

Keywords: Aging, estrous cycle, FSH, IL-10, TNF-α

Öz

Amaç: Bu çalışma, reprodüktif yaşlanma modelleri olarak potansiyellerini değerlendirmek amacıyla, sağlıklı ve yaşlanan fareler arasında östrus döngüsü paternlerini, serum hormon ve sitokin düzeylerini, gen ifadesini ve yumurtalık morfolojisini karşılaştırmayı amaçlamıştır.

Gereç ve Yöntemler: Dokuz aydan büyük dişi BALB/c fareler yaşlı grup olarak kullanıldı ve sağlıklı kontrollerle (6-8 haftalık) karşılaştırıldı. Östrus fazları altı gün boyunca vajinal sitoloji kullanılarak izlendi. Yumurtalık morfolojisi hematoksilen ve eozin boyama ve immünohistokimya kullanılarak

PRECIS: This study demonstrates that aging BALB/c mice exhibit disrupted estrous cycles, ovarian fibrosis, altered cytokine expression, and hormonal changes, supporting their use as a model for reproductive aging.

Corresponding Author/Sorumlu Yazar: Dono Indarto, MD, PhD,
Universitas Sebelas Maret Faculty of Medicine, Department of Physiology; Universitas Sebelas Maret Faculty of Medicine, Biomedical Laboratory, Surakarta, Indonesia
E-mail: dono@staff.uns.ac.id **ORCID ID:** orcid.org/0000-0001-7420-5816

Received/Geliş Tarihi: 17.10.2025 **Accepted/Kabul Tarihi:** 28.01.2026 **Epub:** 17.02.2026 **Publication Date/Yayınlanma Tarihi:** 05.03.2026

Cite this article as: Intan YSN, Soetrisno S, Laqif A, Indarto D. A preliminary investigation of gene expression and levels of FSH, IL-10, and TNF-α and histological staining in natural aging mice. Turk J Obstet Gynecol. 2026;23(1):71-80

analiz edildi. Folikül uyarıcı hormon (FSH), interlökin (IL)-10 ve tümör nekroz faktörü-alfa (TNF-α) serum düzeyleri enzim bağlantılı immünosorbent testi ile ölçüldü. IL-10 ve TNF-α gen ifadesi ters transkripsiyon polimeraz zincir reaksiyonu ile değerlendirildi.

Bulgular: Sağlıklı fareler tüm östrus evrelerinden geçerken, yaşlanan fareler ağırlıklı olarak diöstrus evresinde kaldı ve artmış immün hücre infiltrasyonu ve enflamatuvar değişiklikler sergiledi. Yumurtalık histolojisi, büyüme, fibrozis ve işlevsiz yapıların varlığını gösterdi. Folikül sayısı yaşlanan farelerde azalmış olsa da, bu azalma istatistiksel olarak anlamlı değildi. Serum FSH (1,37±0,20'ye karşı 1,10±0,03 pg/mL) ve TNF-α (37,05±17,31'e karşı 21,57±4,62 pg/mL) anlamlı derecede yükselirken, IL-10 anlamlı derecede azaldı (4,53±0,32'ye karşı 6,23±0,99 pg/mL) (p<0,05). TNF-α mRNA seviyeleri arttı ve IL-10 mRNA seviyeleri azaldı, ancak bu değişiklikler istatistiksel olarak anlamlı değildi.

Sonuç: Yaşlanan BALB/c farelerinde bozulmuş östrus döngüleri, yumurtalık fibrozisi, artmış FSH ve TNF-α ve azalmış IL-10 görülmektedir; bu değişiklikler menopozla ilişkili olanlara benzemektedir. Bu bulgular, yaşlanan BALB/c farelerinin reprodüktif yaşlanma ve terapötik çalışmalar için bir model olarak kullanılmasını desteklemektedir.

Anahtar Kelimeler: Yaşlanma, östrus döngüsü, FSH, IL-10, TNF-α

Introduction

Menopause is a physiological phase that occurs naturally in women with advancing age and is characterized by the permanent cessation of ovarian function and the absence of menstrual cycles for at least 12 consecutive months[1]. Reduced production and circulating levels of estrogen and progesterone lead to metabolic disorders, decreased bone density, and an increased risk of cardiovascular and inflammatory diseases[1,2]. Significant changes occurring during menopause include an increase in systemic inflammation, which contributes to accelerated tissue aging in the ovary[3].

The primary challenge in menopause studies is the complexity of biological changes and the difficulty of studying this process directly in humans, given individual variability and ethical constraints[4]. To advance our understanding of menopause, it is essential to utilize animal models that accurately reflect the biological and molecular changes characteristic of this condition. Rodent models, particularly mice, are widely employed for this purpose due to their physiologically comparable reproductive cycles and the ease with which they can be manipulated and analyzed at the histological and molecular levels[5].

Some animal models of menopause have been developed, but the most commonly used is ovariectomy, in which the ovaries are removed to create an estrogen-deficient condition[6,7]. However, this model neither reflects the ovaries' natural aging process nor demonstrates the gradual changes in the estrous cycle[8]. The ovariectomy model also fails to replicate the chronic inflammation observed during menopause[7,9]. Therefore, naturally aged mice may serve as an alternative model that matches physiological conditions, such as molecular and degenerative changes in the ovaries.

In this study, we used female BALB/c mice aged over nine months as a model of natural aging and compared them with healthy young adult female mice. We evaluated estrous cycle dynamics, levels of follicle-stimulating hormone (FSH) and pro- and anti-inflammatory cytokines [tumor necrosis factor-alpha (TNF-α) and interleukin (IL)-10], expression of inflammation-related mRNAs, and ovarian morphology, assessed by histological and immunohistochemical analyses. This study not only offers an alternative approach to understanding natural reproductive aging but also creates opportunities to develop anti-inflammatory therapeutic interventions targeting menopausal conditions.

Materials and Methods

Research Design

The model employed in this study consisted of female BALB/c mice divided into two groups: Naturally aged mice older than 9 months and healthy young adult females (6-8 weeks old), with five mice per group. All animals were housed in standard laboratory cages and provided ad libitum access to standard feed and drinking water. Environmental conditions were carefully maintained at 26 °C, 50-60% relative humidity, and a 12-hour light/dark cycle to ensure experimental consistency. Healthy young adult mice (6-8 weeks old) underwent a one-week acclimatization period prior to experimental procedures to minimize stress and allow adaptation to the laboratory environment. In contrast, the naturally aging mice older than 9 months had been maintained under laboratory conditions prior to study initiation, and a defined acclimatization or incubation period had not been applied to this group. The study was conducted in accordance with ethical principles for animal research. The protocol was reviewed and approved by the Institutional Review Board/Animal Ethics Committee of Universitas Islam Sultan Agung, Semarang, Indonesia (approval no: 561/XII/2024/Komisi Bioetik, date: 30.12.2024).

Evaluation of Estrous Cycle

The estrous cycle was monitored through vaginal smear cytology for six consecutive days. The smears were collected each morning at the same time to avoid daily hormonal variation. Briefly, a drop of sterile 0.9% NaCl solution was gently instilled into the mouse's vagina to a depth of approximately 0.5-1 cm without causing tissue injury. The fluid was then aspirated, applied to a glass slide[10], air-dried, and subsequently stained with Giemsa (Sigma-Aldrich, USA) according to the manufacturer's protocol[11]. After staining and drying, the slides were examined using a light microscope (Zeiss, Germany) at 100× and 400× magnifications. The estrous cycle phase was determined by observing the dominant cell types (nucleated epithelial cells, cornified epithelial cells, and leukocytes).

Measurements of FSH, IL-10, and TNF-α Levels

According to the kit protocol, IL-10, FSH, and TNF-α levels in mouse serum were measured using the enzyme-linked immunosorbent assay (Elabscience Biotechnology Inc., USA). Blood was collected from mice following cervical dislocation, and serum was separated by centrifugation at 3,000 rpm for 15 minutes. The resulting serum was stored at -80 °C until analysis.

The assay was performed separately for each cytokine and hormone using microtiter plates pre-coated with specific antibodies against IL-10, FSH, and TNF-α (Elabscience, USA). 100 µL of serum or standard solution was added to each well, and the wells were incubated at 37 °C for 90 minutes. After washing, the biotinylated detection antibody solution was added, followed by incubation at 37 °C for 1 hour. After further washing, the horseradish peroxidase-conjugate solution was added and incubated for 30 minutes. 3,3',5,5'-tetramethylbenzidine substrate was then added and incubated until color development occurred, after which the reaction was stopped by adding the stop solution. Absorbance was measured at 450 nm using a microplate reader. Concentrations of IL-10, FSH, and TNF-α were calculated from the standard curve and expressed in pg/mL.

Gene Expression of IL-10 and TNF-α

NA was extracted from ovarian tissues using TRIzol reagent (Invitrogen, Massachusetts, USA) according to the manufacturer's instructions. Approximately 50 mg of tissue was placed into 1 mL of TRIzol, incubated, and then 200 µL of chloroform was added, followed by vigorous shaking for 15 seconds. The mixture was centrifuged at 20,000 × g for 15 minutes at 4 °C, and the upper aqueous phase containing RNA was transferred to a new tube. Isopropanol (0.5 mL per 1 mL of TRIzol) was added, gently mixed, and incubated at room temperature for 10 minutes. After centrifugation at 20,000 × g for 15 minutes, the supernatant was discarded, and the RNA pellet was washed with 75% ethanol and centrifuged at 15,000 × g for 5 minutes. The RNA pellet was dissolved in 100 µL nuclease-free water. RNA concentration and purity were measured on a NanoDrop spectrophotometer (Thermo Fisher Scientific, USA) using absorbance ratios at 260/280 nm and 260/230 nm.

cDNA synthesis was performed using one µg of total RNA with SuperScript II reverse transcriptase (Invitrogen, USA) and oligo(dT) primers, with an initial incubation at 70 °C for 10 minutes, followed by synthesis at 45 °C for 30 minutes. Quantitative reverse transcription polymerase chain reaction (qRT-PCR) was conducted using a PCRmax Eco 48 system (Illumina, USA) with a reaction volume of 20 µL, comprising 10 µL of SYBR Green Master Mix (KAPA Biosystems, Sigma-Aldrich, USA), 1 µL of forward primer, 1 µL of reverse primer, 2 µL of cDNA, and 6 µL of nuclease-free water. Specific primers targeted the IL-10 and TNF-α genes, with glyceraldehyde-3-phosphate dehydrogenase (GAPDH) as the reference gene. The thermal cycling protocol included an initial denaturation at 95 °C for 3 minutes, followed by 40 cycles of denaturation at 95 °C for 15 seconds and annealing/extension at 60 °C for 1 minute. Gene expression levels were determined based on cycle threshold values and analyzed using Eco v5.0 software (Illumina, USA). Relative expression was calculated using the 2^−ΔΔCt (Livak) method, normalized to GAPDH, and results were presented as fold changes relative to the healthy group.

Ovary Histology

Ovarian tissues were collected and carefully examined for macroscopic features. Each ovary was photographed to document gross morphology prior to histological processing. For microscopic examination, 3-4 µm-thick ovarian tissue sections were cut from paraffin blocks, dried at 37 °C, and heated on a slide warmer at 60 °C. Deparaffinization was performed by sequentially immersing the tissue sections in three xylene solutions (Xylol I, II, and III) (Sigma-Aldrich, St. Louis, Missouri, USA), followed by rehydration through a graded series of alcohol solutions (absolute, 96%, and 80%). The slides were then rinsed with running water.

Tissue staining was conducted using hematoxylin and eosin (H&E). The slides were first immersed in hematoxylin solution (Sigma-Aldrich, St. Louis, Missouri, USA) to stain the cell nuclei and were then rinsed with running water. Next, eosin (Sigma-Aldrich, St. Louis, Missouri, USA) was applied to stain the cytoplasm and other tissue structures, and the slides were rinsed again. The bluing process was performed using Tacha Bluing solution (Biocare Medical, California, USA), followed by a final rinse with water.

The slides then underwent gradual dehydration in graded alcohols (80% and 96%) and were cleared using xylene (Xylol I, II, and III). The mounting process was performed using Ecomount (Biocare Medical, California, USA) and was covered with a coverslip. The stained ovarian tissue preparations were observed under a light microscope (Olympus, Germany) at 100× magnification in five fields of view.

Statistical Analysis

Data were analyzed using SPSS software. One-way analysis of variance was performed, followed by a post hoc least significant difference test. Results were presented as mean ± standard deviation, with the significance level at $p<0.05$.

Results

Mice Vaginal Cytology

Vaginal smear cytology illustrates the cellular composition of the vaginal epithelium across the four phases of the estrous cycle, highlighting the morphological changes that reflect hormonal fluctuations and tissue activity in each phase. Figure 1A shows the proestrus phase, characterized by a predominance of nucleated epithelial cells with some cornified cells, indicating

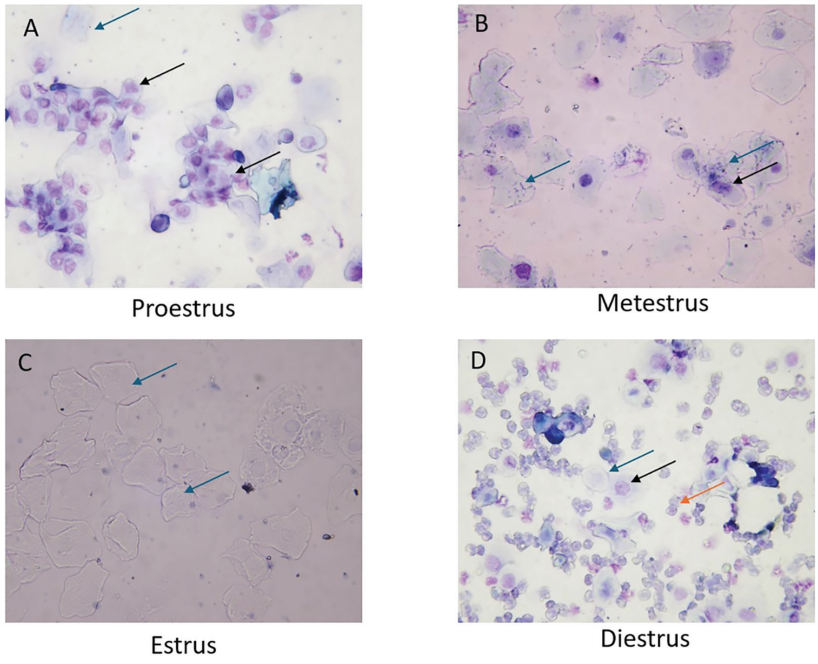

Figure 1. Vaginal smear cytology in different estrous cycle phases in mice. Black arrows indicate nucleated epithelial cells, blue arrows indicate cornified epithelial cells, and orange arrows indicate immune cells. (A) In the proestrus phase, nucleated epithelial cells (black arrows) and cornified epithelial cells (blue arrows) are observed, with nucleated cells being dominant. (B) Only cornified epithelial cells (blue arrows) are present during the estrus phase. (C) In the metestrus phase, cornified epithelial cells (blue arrows) are still visible, but nucleated epithelial cells (black arrows) begin to reappear. (D) In the diestrus phase, a mixture of nucleated epithelial cells (black arrows), cornified epithelial cells (blue arrows), and immune cells (orange arrows) is observed

epithelial proliferation in response to estrogen stimulation, without complete keratinization. Figure 1B depicts the estrus phase, marked by fully cornified epithelial cells, reflecting complete keratinization under maximal estrogen influence, coinciding with the peak of sexual receptivity. Figure 1C shows the metestrus phase, characterized by dominance of cornified cells and the reappearance of nucleated epithelial cells. This pattern indicates a decline in estrogen levels, an increase in progesterone levels, and the initiation of epithelial regeneration. Figure 1D displays the diestrus phase, in which nucleated epithelial cells, cornified epithelial cells, and immune cells are observed. This reflects progesterone dominance, immune-mediated tissue remodeling, and the resting phase before the cycle begins anew.

Estrous Cycle in Mice

The estrous cycle graph comparing healthy and aging mice shows differences in hormonal patterns over a 6-day observation period, as illustrated in Figure 2A. In healthy mice (represented by circle symbols), the estrous cycle shows a regular phase transition from day to day. The dynamic changes from proestrus to estrus, metestrus, and diestrus reflect a normal, cyclical reproductive pattern influenced by regular fluctuations in estrogen and progesterone. In contrast, aged mice (represented by square symbols) spent most of the observation period in the diestrus phase. Diestrus is generally the resting phase in the estrous cycle, characterized by low estrogen levels and the absence of ovulation. The prolonged diestrus phase in aging mice indicates that ovarian follicles no longer develop and ovulation does not occur. This is a hallmark of reproductive aging, characterized by the decline or cessation of ovarian function, which resembles the physiological condition of menopause in humans.

The doughnut diagram in Figure 2B visually emphasizes this difference. In healthy mice, the distribution of time spent in each of the four estrous phases, proestrus, estrus, metestrus, and diestrus, appears relatively balanced. This balanced phase distribution reflects a regular estrous cycle and active endocrine signaling. However, in aging mice, the diagram is dominated by the light gray color representing the diestrus phase, indicating that most of the time is spent in this non-reproductive phase. This change reflects a significant decline in ovarian activity due to disrupted or weakened hormonal signaling, particularly in estrogen production.

Histological analysis of vaginal smears further supports these findings. In healthy mice during the estrus phase, as shown in Figure 2C, the epithelial layer is dominated by cornified epithelial cells (blue arrows), which are flattened, anucleate cells resulting from complete keratinization of the epithelium. This cellular profile is characteristic of the estrous phase, when estrogen levels peak, stimulating epithelial maturation and preparing the reproductive tract for potential

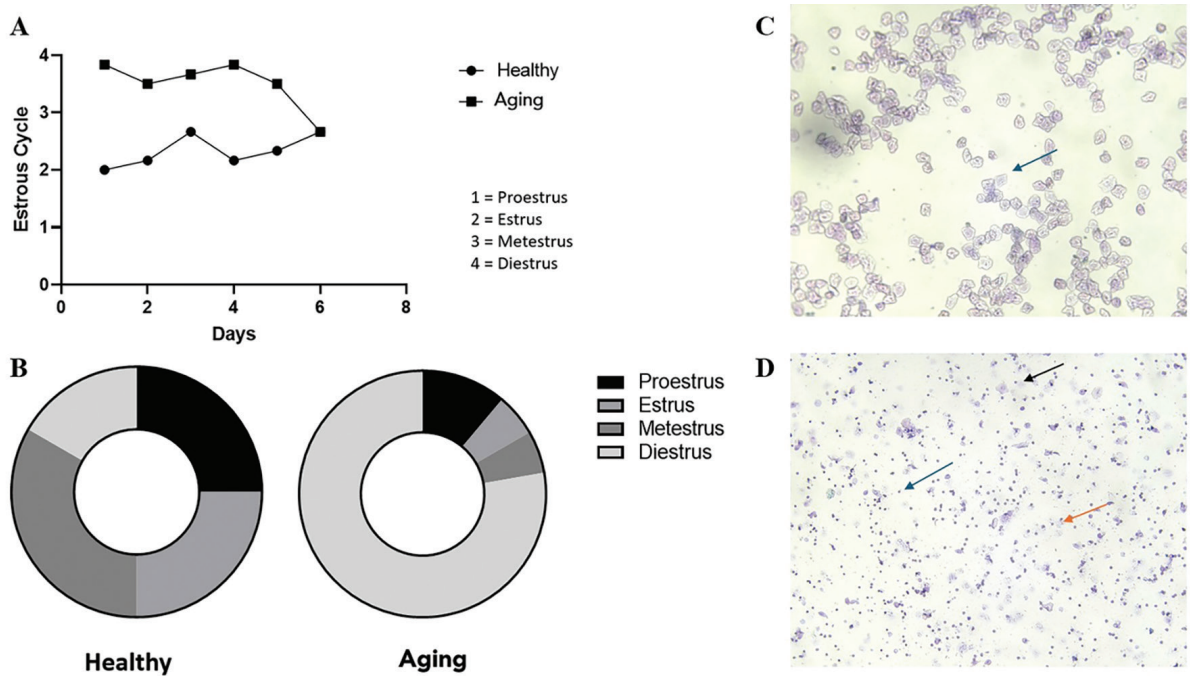

Figure 2. Observation of estrous cycle in healthy and aging mice. (A) The estrous cycle graph of healthy and aging mice shows that during the 6-day observation period, healthy mice undergo regular estrous phase transitions. (B) Donut diagram of estrous phase distribution in healthy and aging mice. (C) In healthy mice during the estrus phase, numerous cornified epithelial cells are observed (indicated by blue arrows). (D) Aging mice show fewer cornified epithelial cells, more nucleated epithelial cells (black arrows), and immune cells (orange arrows)

fertilization. The absence of immune cells during this phase indicates the lack of inflammation, consistent with an optimal physiological reproductive state. However, in aging mice, the cellular composition appears markedly different. Figure 2D shows fewer cornified epithelial cells, whereas nucleated epithelial cells (black arrows) and immune cells (orange arrows) are more numerous. Nucleated cells indicate incomplete keratinization, a sign of insufficient estrogen stimulation. Meanwhile, the increased number of immune cells reflects tissue remodeling or mild inflammation, possibly in response to epithelial regression in the reproductive tract resulting from decreased ovarian hormone production. These cytological findings align with the hormonal and behavioral signs of menopause in rodents and serve as reliable indicators for assessing reproductive aging[6].

Cellular and Tissue Morphology of Mice Ovary

During the aging transition, significant changes occur in ovarian morphology due to altered hormonal regulation and tissue remodeling processes[1]. In aging mice, the ovaries appear larger than those of healthy mice. As shown in Figure 3, this enlargement may be caused by the accumulation of non-functional structures such as fibrotic tissue, cysts, residual follicles, and stromal tissue. These structural abnormalities are most likely the result of hormonal imbalances and degenerative processes associated with aging.

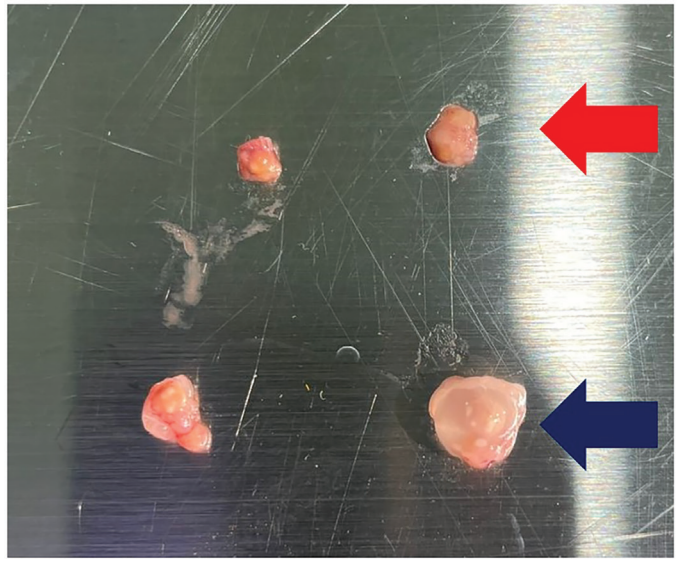

Figure 3. The macroscopic appearance of ovaries in healthy mice (red arrow) and aging mice (blue arrow) shows differences in organ size

Histological analysis of ovarian tissue from aging mice revealed differences in follicle number and types compared with the healthy group. The healthy group exhibited a greater number of follicles at various developmental stages, particularly primary, secondary, and antral follicles (Figure 4B).

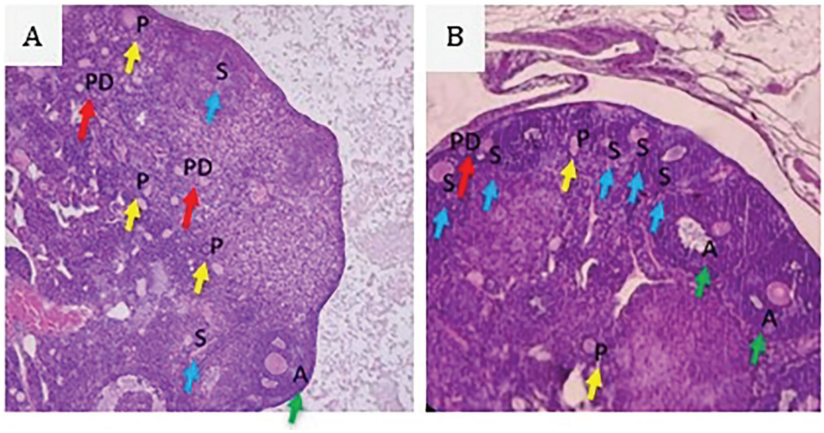

Figure 4. Results of hematoxylin and eosin staining assay show various stages of ovarian follicle development in mice, namely primordial follicles (yellow arrows), primary follicles (red arrows), secondary follicles (blue arrows), and antral follicles (green arrows). (A) Aging mice show fewer secondary and antral follicles compared to healthy mice. (B) Healthy mice show a higher number of secondary and antral follicles compared to aging mice

By contrast, in the aging group the total number of follicles decreased, with a predominance of early-stage follicles (primordial and primary), whereas secondary and antral follicles were rare or undetectable (Figure 4A).

The number of each follicle type was lower in the aging group than in the healthy group, although the differences were not statistically significant (Figure 5). This downward trend remains consistent with the histological appearance of aging ovaries (Figure 4), in which the process of follicular atresia progresses more rapidly than follicular recruitment and maturation proceed. This condition leads to menopausal ovaries that are dominated by primordial and primary follicles that fail to develop into the secondary and antral stages[12].

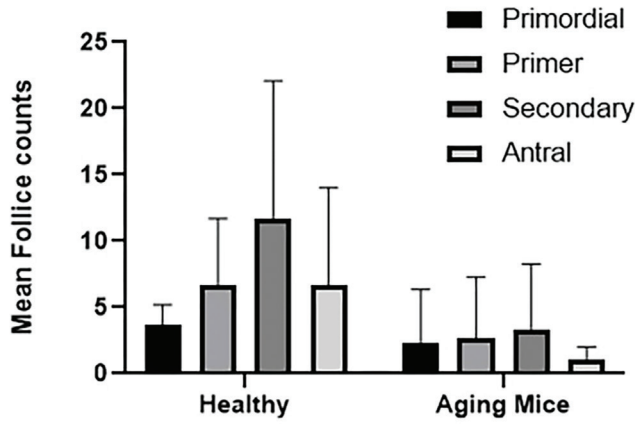

Figure 5. The total number of follicles in healthy and aging mice. The number of follicles decreased in aging mice due to the degeneration of ovarian function. Data are presented as mean ± standard deviation

FSH, TNF-α, and IL-10 Level in Mice Serum

To investigate differences in hormonal imbalances and systemic inflammation between healthy and aging mice, we measured serum levels of FSH, IL-10, and TNF-α. As shown in Figure 6A, serum FSH levels were significantly higher in aged mice (1.37±0.20 pg/mL) than in healthy controls (1.10±0.03 pg/mL) ($p<0.05$). This elevation in FSH is a well-established hallmark of menopause, reflecting the diminished negative feedback from ovarian hormones such as estrogen, which typically decline with ovarian aging. Additionally, Figure 6B illustrates that serum TNF-α, a pro-inflammatory cytokine, was significantly increased in aging mice (37.05±17.31 pg/mL) compared with healthy mice (21.57±4.62 pg/mL) ($p<0.05$). This finding indicates heightened systemic inflammation in aging mice, consistent with the low-grade chronic inflammatory state often associated with reproductive aging. In contrast, as shown in Figure 6C, serum IL-10 levels, an anti-inflammatory cytokine, were significantly reduced in aging mice (4.53±0.32 pg/mL) compared to healthy controls (6.23±0.99 pg/mL) ($p<0.05$). The decrease in IL-10 may contribute to the imbalance between pro- and anti-inflammatory signaling, further supporting the presence of an inflammatory state during menopause.

Expression of TNF-α and IL-10 in Mice Ovary

qRT-PCR analysis assessed the differences in mRNA expression levels of TNF-α and IL-10 between healthy and aging mice. As shown in Figure 7A, TNF-α mRNA expression was significantly increased in aged mice (4.75±2.21) compared with healthy mice (1.06±0.53; $p<0.05$), indicating an upregulation of pro-inflammatory gene expression associated with aging. Conversely, Figure 7B shows that IL-10 mRNA expression was lower in aged mice (0.45±0.22) than in healthy mice (1.02±0.69); however, this difference was not statistically significant. This trend suggests a possible decline in anti-inflammatory signaling in aging mice, consistent

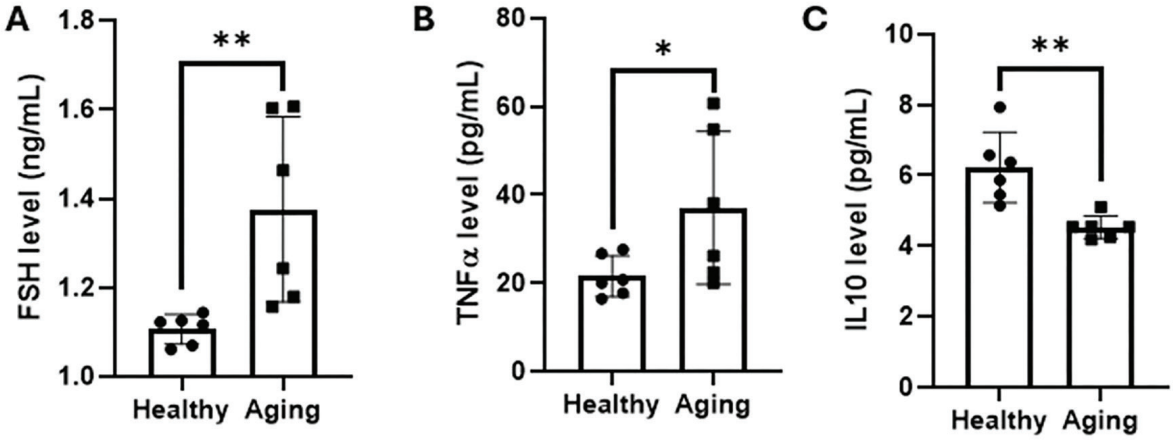

Figure 6. Differences in serum levels of FSH, TNF-α, and IL-10 between healthy and aging mice. (A) There was a significant difference between the healthy and aging mouse groups ($p<0.05$), with serum FSH levels markedly higher in aging mice than in healthy mice. (B) There was a significant difference between the healthy and aging mouse groups ($p<0.05$), with a significant increase in serum TNF-α levels in aging mice compared to healthy mice. (C) There was a significant difference between the healthy and aging mouse groups ($p<0.05$), with a clear reduction in serum IL-10 levels in aging mice compared to healthy mice. Significance indicators: *: $p<0.05$; **: $p<0.01$

FSH: Follicle-stimulating hormone, IL-10: Interleukin-10, TNF-α: Tumor necrosis factor-alpha

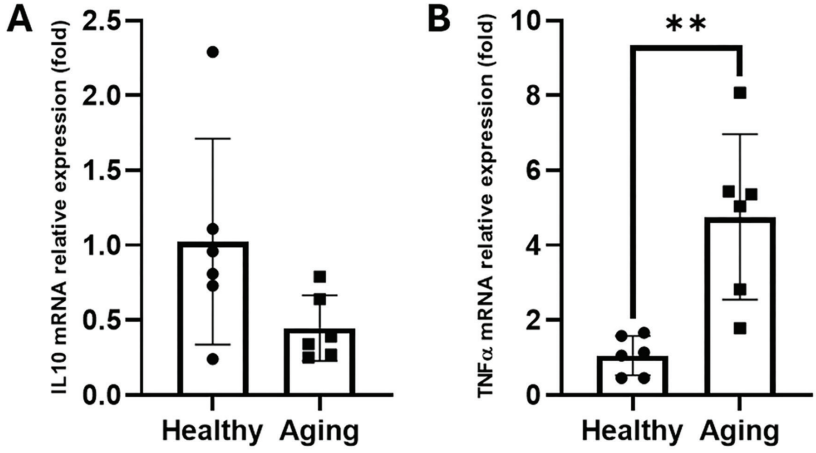

Figure 7. Differences in TNF-α and IL-10 mRNA expression between healthy and aging mice. (A) There was a significant difference between the healthy and aging mice groups ($p<0.05$), with a significant increase in TNF-α mRNA expression in aging mice compared to healthy mice. (B) There was no significant difference between the healthy and aging mouse groups ($p>0.05$). However, IL-10 mRNA expression decreased in aging mice compared to healthy mice, although this difference was not statistically significant Significance indicators: **: p<0.0

IL-10: Interleukin-10, TNF-α: Tumor necrosis factor-alpha 1

with a shift towards a more pro-inflammatory environment, despite the absence of a statistically significant difference. These findings support the serum cytokine level results and further strengthen the hypothesis that menopause may lead to transcriptional changes that contribute to systemic inflammation.

Discussion

This study demonstrates that aged female BALB/c mice (>9 months of age) exhibit physiological and molecular changes resembling human menopause. The key findings indicate that the diestrus phase predominates in the estrous cycle and is characterized by increased levels of FSH and TNF-α, decreased levels of IL-10, and structural changes in the ovaries. These results confirm that this model effectively represents menopause. Estrous cycle analysis revealed that aging mice primarily remained in the diestrus phase and exhibited immune cells and nucleated epithelial cells. In contrast, healthy mice displayed dynamic transitions between estrous phases. These observations are consistent with previous

studies reporting that aged mice experience disrupted estrous cycles and tend to remain in diestrus due to declining ovarian activity[13,14]. However, estrous cycle monitoring was limited to six consecutive days, which is shorter than the 14-20 days commonly recommended to define persistent diestrus[15]. Therefore, the conclusion regarding estrous cycle disruption should be interpreted with caution, and longer monitoring is needed in future studies.

The significant increase in FSH levels observed in aging mice in this study reflects the disruption of ovarian hormonal feedback, particularly the decline in estrogen with age[16]. Previous studies have reported that mice with aging ovaries exhibit surges in FSH, which serve as key indicators of endocrine dysfunction associated with menopause[17]. Concurrently, increased TNF-α and decreased IL-10 levels observed in aging mice in this study indicate an immune imbalance leading to a systemic pro-inflammatory state. These findings are consistent with earlier studies showing that aging rats exhibit elevated expression of pro-inflammatory cytokines (such as TNF-α and IL-6) and reduced expression of anti-inflammatory cytokines (such as IL-10), reflecting the low-grade chronic inflammation characteristic of menopause[18-20].

Furthermore, the increased TNF-α mRNA expression and decreased IL-10 mRNA expression in aging mice in this study suggest transcriptional regulatory changes in immune-related genes. Although the decrease in IL-10 expression was not statistically significant, the observed direction of change aligns with a shift toward a systemic pro-inflammatory state. However, given the limited estrous monitoring duration and small sample size, these molecular changes should be regarded as indicative rather than definitive. Previous studies have found that the ovaries of aging rats exhibit increased expression of pro-inflammatory genes and decreased anti-inflammatory regulators, contributing to tissue damage and oxidative stress[18,21,22].

The natural aging model used in this study offers advantages over the ovariectomized (OVX) model for evaluating anti-inflammatory therapeutic strategies. In contrast to OVX, which induces an abrupt and artificial loss of ovarian hormones, natural aging is characterized by a gradual decline in ovarian function, accompanied by progressive endocrine and immune alterations[23]. The concurrent increase in TNF-α and decrease in IL-10 observed in aging mice reflect a chronic, low-grade inflammatory state rather than an acute inflammatory response arising from natural aging processes, whereas OVX-induced low-grade inflammation occurs through immune cell-driven mechanisms that are distinct from the age-associated inflammatory pathways[23,24]. Ovary-intact aging models preserve residual ovarian tissue and ongoing immune-endocrine interactions, which more accurately reflect the physiological and molecular features of human menopause, including anestrus and reduced gonadal steroid levels[25].

Morphological observations revealed changes in the ovaries of mice. Aged mice exhibited enlarged ovaries containing non-functional lesions, including fibrotic tissue and cysts, indicating tissue degeneration due to chronic hormonal imbalance. Previous studies have shown that the ovaries of aged mice exhibit increased fibrosis, decreased numbers of mature follicles, and stromal accumulation due to reduced estrogenic activity and increased oxidative stress[26-28]. Additionally, H&E analysis showed a reduction in the number of follicles in aging mice compared with healthy mice. These findings are consistent with previous research demonstrating an age-related decline in ovarian follicle numbers in Egyptian spiny mice[29]. With advancing age, the number of ovarian follicles in women decreases due to follicular atresia and ovulation[29]. This reduction is accompanied by a decline in the number of ovarian granulosa cells, which are the leading producers of estradiol and inhibin B. Levels of anti-Müllerian hormone (AMH), also produced by granulosa cells, similarly decrease. The diminished production of estrogen and inhibins A and B leads to the loss of inhibition of gonadotropin secretion, resulting in increased FSH and luteinizing hormone levels[30]. This reduction in estrogen levels also disrupts the balance of the hypothalamic-pituitary-ovarian axis[31]. As a result, endometrial development fails, leading to irregular menstrual cycles and, eventually, complete cessation of menstruation (menopause)[1,32].

Study Limitations

The molecular scope of this study was limited to IL-10 and TNF-α and did not include other important inflammatory and hormonal markers, such as IL-6, estradiol, and AMH, which could provide a more comprehensive understanding of reproductive aging. Although the histological analyses successfully revealed ovarian changes, more detailed molecular and ultrastructural assessments would strengthen the interpretation of tissue degeneration. The small sample size (n=5 per group) represents a major limitation; the findings should be interpreted with caution. Moreover, estrous cycle monitoring was limited to six days, which is insufficient to definitively establish persistent cycle arrest. Finally, caution is needed when extrapolating these findings to humans, as physiological differences between the estrous cycle in mice and the menstrual cycle in women may limit direct comparability.

Conclusion

Our findings indicate that aged female mice exhibit physiological and molecular signs of menopause, making them suitable models for experimental studies of reproductive aging and for the development of therapeutic interventions targeting inflammation and ovarian dysfunction associated with menopause.

Ethics

Ethics Committee Approval: The protocol was reviewed and approved by the Institutional Review Board/Animal Ethics Committee of Universitas Islam Sultan Agung, Semarang, Indonesia (approval no: 561/XII/2024/Komisi Bioetik, date: 30.12.2024).
Informed Consent: Not necessary.

Footnotes

Authorship Contributions

Surgical and Medical Practices: S.S., Concept: Y.S.N.I., D.I., Design: Y.S.N.I., S.S., Data Collection or Processing: Y.S.N.I., A.L., Analysis or Interpretation: Y.S.N.I., A.L., D.I., Literature Search: S.S., Writing: Y.S.N.I., A.L., D.I.
Conflict of Interest: No conflict of interest was declared by the authors.
Financial Disclosure: The authors declared that this study received no financial support.

References

1. Peacock K, Carlson K, Ketvertis KM. Menopause [Internet]. In: StatPearls. Treasure Island (FL): StatPearls Publishing; 2025 [cited 2025 June 12]. Available from: http://www.ncbi.nlm.nih.gov/books/NBK507826/
2. Santoro N, Roeca C, Peters BA, Neal-Perry G. The menopause transition: signs, symptoms, and management options. J Clin Endocrinol Metab. 2021;106:1-15.
3. McCarthy M, Raval AP. The peri-menopause in a woman's life: a systemic inflammatory phase that enables later neurodegenerative disease. J Neuroinflammation. 2020;17:317.
4. Barber K, Charles A. Barriers to accessing effective treatment and support for menopausal symptoms: a qualitative study capturing the behaviours, beliefs and experiences of key stakeholders. Patient Prefer Adherence. 2023;17:2971-80.
5. Koebele SV, Bimonte-Nelson HA. Modeling menopause: the utility of rodents in translational behavioral endocrinology research. Maturitas. 2016;87:5-17.
6. Diaz Brinton R. Minireview: translational animal models of human menopause: challenges and emerging opportunities. Endocrinology. 2012;153:3571-8.
7. Oishi Y, Manabe I. Macrophages in age-related chronic inflammatory diseases. Npj Aging Mech Dis. 2016;2:16018.
8. Brinton RD. Investigative models for determining hormone therapy-induced outcomes in brain: evidence in support of a healthy cell bias of estrogen action. Ann N Y Acad Sci. 2005;1052:57-74.
9. Gilmer G, Bean AC, Iijima H, Jackson N, Thurston RC, Ambrosio F. Uncovering the "riddle of femininity" in osteoarthritis: a systematic review and meta-analysis of menopausal animal models and mathematical modeling of estrogen treatment. Osteoarthritis Cartilage. 2023;31:447-57.
10. Quignon C. Collection and analysis of vaginal smears to assess reproductive stage in mice. Curr Protoc 2023;3:e887.
11. Musyayyadah H, Wulandari F, Nangimi AF, Anggraeni AD, Ikawati M, Meiyanto E. The growth suppression activity of diosmin and PGV-1 co-treatment on 4T1 breast cancer targets mitotic regulatory proteins. Asian Pac J Cancer Prev APJCP. 2021;22:2929-38.
12. Park SU, Walsh L, Berkowitz KM. Mechanisms of ovarian aging. Reprod Camb Engl. 2021;162:R19-33.
13. Umehara T, Winstanley YE, Andreas E, Morimoto A, Williams EJ, Smith KM, et al. Female reproductive life span is extended by targeted removal of fibrotic collagen from the mouse ovary. Sci Adv. 2022;8:eabn4564.
14. Herrera-Pérez JJ, Hernández-Hernández OT, Flores-Ramos M, Cueto-Escobedo J, Rodr´guez-Landa JF, Mart´nez-Mota L. The intersection between menopause and depression: overview of research using animal models. Front Psychiatry [Internet] 2024 [cited 2025 June 25];15. Available from: https://www.frontiersin.org/journals/psychiatry/articles/10.3389/fpsyt.2024.1408878/full
15. Quignon C. Collection and analysis of vaginal smears to assess reproductive stage in mice. Curr Protoc. 2023;3:e887.
16. Spicer J, Malaspina D, Blank SV, Goosens KA. Follicle-stimulating hormone: more than a marker for menopause: FSH as a frontier for women's mental health. Psychiatry Res. 2025;345:116239.
17. Xiong J, Kang SS, Wang M, Wang Z, Xia Y, Liao J, et al. FSH and ApoE4 contribute to Alzheimer's disease-like pathogenesis via C/EBPβ/δ-secretase in female mice. Nat Commun. 2023;14:6577.
18. Lliberos C, Liew SH, Zareie P, La Gruta NL, Mansell A, Hutt K. Evaluation of inflammation and follicle depletion during ovarian ageing in mice. Sci Rep. 2021;11:278.
19. Zhu Z, Xu W, Liu L. Ovarian aging: mechanisms and intervention strategies. Med Rev (2021). 2022;2:590-610.
20. Ameho S, Klutstein M. The effect of chronic inflammation on female fertility. Reprod Camb Engl. 2025;169:e240197.
21. Wu Y, Li M, Zhang J, Wang S. Unveiling uterine aging: much more to learn. Ageing Res Rev. 2023;86:101879.
22. Isola JVV, Hense JD, Osório CAP, Biswas S, Alberola-Ila J, Ocañas SR, et al. Reproductive ageing: Inflammation, immune cells, and cellular senescence in the aging ovary. 2024 [cited 2025 June 25]; Available from: https://rep.bioscientifica.com/view/journals/rep/168/2/REP-23-0499.xml
23. Zakaria R, Said RM, Othman Z, Azman KF, Aziz CBA. Menopause rodent models: suitability for cognitive aging research. Int Med J. 2019;26:450-2.
24. Benedusi V, Martini E, Kallikourdis M, Villa A, Meda C, Maggi A. Ovariectomy shortens the life span of female mice. Oncotarget. 2015;6:10801-11.
25. McCarthy M, Raval AP. The peri-menopause in a woman's life: a systemic inflammatory phase that enables later neurodegenerative disease. J Neuroinflammation. 2020;17:317.
26. Briley SM, Jasti S, McCracken JM, Hornick JE, Fegley B, Pritchard MT, et al. Reproductive age-associated fibrosis in the stroma of the mammalian ovary. Reprod Camb Engl. 2016;152:245-60.
27. Zhang Z, Schlamp F, Huang L, Clark H, Brayboy L. Inflammaging is associated with shifted macrophage ontogeny and polarization in the aging mouse ovary. 2020 [cited 2025 June 25]; Available from: https://rep.bioscientifica.com/view/journals/rep/159/3/REP-19-0330.xml
28. Guo Y, Xue L, Tang W, Xiong J, Chen D, Dai Y, et al. Ovarian microenvironment: challenges and opportunities in protecting against chemotherapy-associated ovarian damage. Hum Reprod Update. 2024;30:614-47.

29. Bellofiore N, George E, Vollenhoven B, Temple-Smith P. Reproductive aging and menopause-like transition in the menstruating spiny mouse (Acomys cahirinus). Hum Reprod Oxf Engl. 2021;36:3083-94.
30. Hall JE. Endocrinology of the menopause. Endocrinol Metab Clin North Am. 2015;44:485-96.
31. Tanbo TG, Fedorcsak PZ. Can time to menopause be predicted? Acta Obstet Gynecol Scand. 2021;100:1961-8.
32. McNeil MA, Merriam SB. Menopause. Ann Intern Med. 2021;174:ITC97-112.